Structural effects of Parkinson's disease linked DJ-1 mutations

GAETANO MALGIERI AND DAVID ELIEZER

Department of Biochemistry and Program in Structural Biology, Weill Cornell Medical College, New York, New York 10021, USA

(RECEIVED December 17, 2007; FINAL REVISION February 12, 2008; ACCEPTED February 18, 2008)

Abstract

Mutations in the protein DJ-1 are associated with familial forms of Parkinson's disease, indicating that DJ-1 may be involved in pathways related to the etiology of this disorder. Here we have used solution state NMR and circular dichroism spectroscopies to evaluate the extent of structural perturbations associated with five different Parkinson's disease linked DJ-1mutations: L166P, E64D, M26I, A104T, and D149A. Comparison of the data with those obtained for the wild-type protein shows that the L166P mutation leads to severe and global destabilization and unfolding of the protein structure, while the structure of the E64D mutation, as expected, is nearly unperturbed. Interestingly, the remaining three mutants all show different degrees of structural perturbation, which are accompanied by a reduction in the thermodynamic stability of the protein. The observed structural and thermodynamic differences are likely to underlie any functional variations between these mutants and the wild type, which in turn are likely responsible for the pathogenicity of these mutations.

Keywords: Parkinson's disease; DJ-1; protein structure; protein stability; NMR; circular dichroism

Supplemental material: see www.proteinscience.org

Over the course of the past decade, dramatic advances have been made in the identification of genes associated with familial forms of Parkinson's disease (PD). Although familial PD is relatively rare compared with idiopathic disease, the associated genes provide an opportunity to gain important insights into molecular pathways that lead to Parkinsonism and that may be important in sporadic forms of this syndrome as well. Currently, as many as 11 genetic loci (PARK 1/4, 2, 5–8, and 9–13) with linkages to PD have been established, and for six of these (PARK 1/4, 2, 6, 7, 8, and 9), the responsible gene has been identified and conclusively determined to cause familial forms of PD (Polymeropoulos et al. 1997; Kitada et al. 1998; Bonifati et al. 2003; Paisan-Ruiz et al. 2004; Valente et al. 2004; Zimprich et al. 2004; Ramirez et al. 2006).

PARK7 was identified as a 24-kb gene that encodes a 189-amino-acid multifunctional protein, DJ-1 (Bonifati et al. 2003), and several point mutations in this gene have been associated with an autosomal recessive early onset form of PD (Abou-Sleiman et al. 2003; Bonifati et al. 2003; Hague et al. 2003; Hering et al. 2004; Annesi et al. 2005; Tang et al. 2006). Because of the recessive nature of DJ-1–associated PD, it is considered likely that the development of the disease is due to the loss of function of this protein, yet this function remains poorly understood. Analysis of both the primary amino acid sequence (Wagenfeld et al. 1998; Hod et al. 1999) and the high-resolution structure of DJ-1 (Honbou et al. 2003; Huai et al. 2003; Lee et al. 2003; Tao and Tong 2003; Wilson et al. 2003) indicated that the protein belongs to the ThiJ/PfpI/GAT protein superfamily, which includes proteins with such diverse functions as kinase, protease, catalase, amidotransferase, and chaperone activities.

Reprint requests to: David Eliezer, Department of Biochemistry and Program in Structural Biology, Weill Cornell Medical College, 1300 York Avenue, New York, NY 10021, USA; e-mail: dae2005@med.cornell.edu; fax: (212) 746-4843.

Article and publication are at http://www.proteinscience.org/cgi/doi/10.1110/ps.073411608.

In vitro, a very weak proteolytic activity was reported for DJ-1 (Olzmann et al. 2004) but other studies failed to detect such activity (Lee et al. 2003; Wilson et al. 2003; Shendelman et al. 2004) and the high-resolution structure of the protein revealed the absence of a properly organized catalytic triad. In PfpI-type proteases, a Cys/His/Glu catalytic triad is formed at an inter-subunit interface that is absent in the DJ-1 dimer and is possibly prevented from forming by the presence of DJ-1 α-helix 8, which is absent in PfpI-like domains. Thus, it appears that DJ-1 is not an effective protease in vitro, but it remains possible that the isolated protein adopts an inhibited conformation that may be subject to activation and regulation in vivo. An in vitro chaperone activity was also reported for DJ-1 based on its ability to inhibit the aggregation of proteins such as citrate synthase, firefly luciferase, GST, and the PD-linked protein α-synuclein (Lee et al. 2003; Shendelman et al. 2004; Zhou et al. 2006). Chaperone activity was found to be restricted to mildly oxidized forms of DJ-1, with the responsible oxidation site being reported as either Cys 53 (Shendelman et al. 2004) or Cys 106 (Zhou et al. 2006). Although a separate study failed to reproduce DJ-1 chaperone activity for citrate synthase (Olzmann et al. 2004), this may have been due to the use of either under- or over-oxidized forms of the protein.

DJ-1 has also been proposed to function in oxidative stress response pathways, based in part on its identification as a protein that is sensitive to both exogenously (hydrogen peroxide and paraquat) and endogenously (lipopolysaccharide-mediated reactive oxidative species production) induced oxidative stress, both of which lead to the appearance of a low PI (5.8) form of the protein in cultured cells (Mitsumoto and Nakagawa 2001; Mitsumoto et al. 2001). The low PI form of the protein was demonstrated to result from oxidation of Cys 106 in cells exposed to oxidative stress (paraquat and MPP^+) (Canet-Aviles et al. 2004), and rotenone exposure also led to the formation of the low PI form of the protein both in cultured cells and in rats (Betarbet et al. 2006). DJ-1 knockdown in cell culture also resulted in increased sensitivity to oxidizing reagents (Martinat et al. 2004; Taira et al. 2004), and more recently, loss of functional DJ-1 in both fly (Lavara-Culebras and Paricio 2007) and mouse models (Kim et al. 2005; Andres-Mateos et al. 2007) implied a role for DJ-1 in resistance to oxidative stress. In vitro, DJ-1 has also been shown to be capable of scavenging H_2O_2 (Canet-Aviles et al. 2004; Taira et al. 2004; Andres-Mateos et al. 2007), suggesting a peroxiredoxin-like peroxidase activity. In light of the evidence for DJ-1 acting in oxidative stress response pathways, a loss of function of the protein might be expected to lead to cell toxicity through an increased susceptibility to oxidative damage.

A number of different DJ-1 point mutations have been potentially associated with familial PD and might therefore be expected to lead to a loss of function of the protein. Among these are the initially identified L166P lesion (Bonifati et al. 2003), as well as the mutations M26I and D149A (Abou-Sleiman et al. 2003), A104T (Hague et al. 2003), and E64D (Hering et al. 2004). The location of these mutants is indicated in the primary sequence of the protein, as well as on its three-dimensional structure, in Figure 1. The structural and functional effects of the L166P mutation have been characterized most thoroughly. In vitro, this mutation leads to a drastic reduction in the secondary structure content of the protein and the absence of any thermal melting behavior (Olzmann et al. 2004; Shendelman et al. 2004), strongly suggesting that the structure of the mutant protein is severely perturbed. Accordingly, the L166P mutant is found as a monomer in solution (Tao and Tong 2003; Olzmann et al. 2004) and is also unable to function as a chaperone (Shendelman et al. 2004) or a protease (Olzmann et al. 2004) in vitro. In cell culture, the L166P mutant is expressed at much lower steady-state levels than the wild-type protein and exhibits a greatly increased turnover rate (Macedo et al. 2003; Gorner et al. 2004; Olzmann et al. 2004). These effects are partially, but not fully abrogated by proteasome inhibitors (Miller et al. 2003; Moore et al. 2003; Gorner et al. 2004; Olzmann et al. 2004) and the L166P, but not wild-type, protein is polyubiquitnated (Olzmann et al. 2004), implying a role for the ubiquitin/proteasome system in the turnover of this mutant, although other degradation pathways are likely involved as well. L166P DJ-1 is also ineffective in eliminating H_2O_2 within cells (Taira et al. 2004) or protecting cells from death induced by H_2O_2 (Gorner et al. 2004; Martinat et al. 2004; Taira et al. 2004; Kim et al. 2005).

In contrast to the relative wealth of information available for the L166P mutation, fewer reports have appeared describing the structural and functional effects of the four abovementioned PD-linked DJ-1 mutations. The E64D mutation represents a highly conservative mutation on the surface of the protein, consistent with a crystal structure that is nearly identical to that of the wild-type protein (Hering et al. 2004). In cells, transfected E64D DJ-1 is highly stable, although steady-state expression levels are slightly less than those of the wild-type protein (Hering et al. 2004), and turnover rates appear to be slightly higher (Gorner et al. 2004). For A104T and D149A, steady-state expression levels in cell culture have been reported to be slightly decreased compared with the wild-type protein, while M26I expression levels are dramatically decreased, though still not as much as for the L166P mutant (Blackinton et al. 2005). The M26I mutant also exhibits a significantly increased rate of turnover, though again this effect is not nearly as strong as for the L166P mutant (Blackinton et al. 2005). The A104T, D149A, and

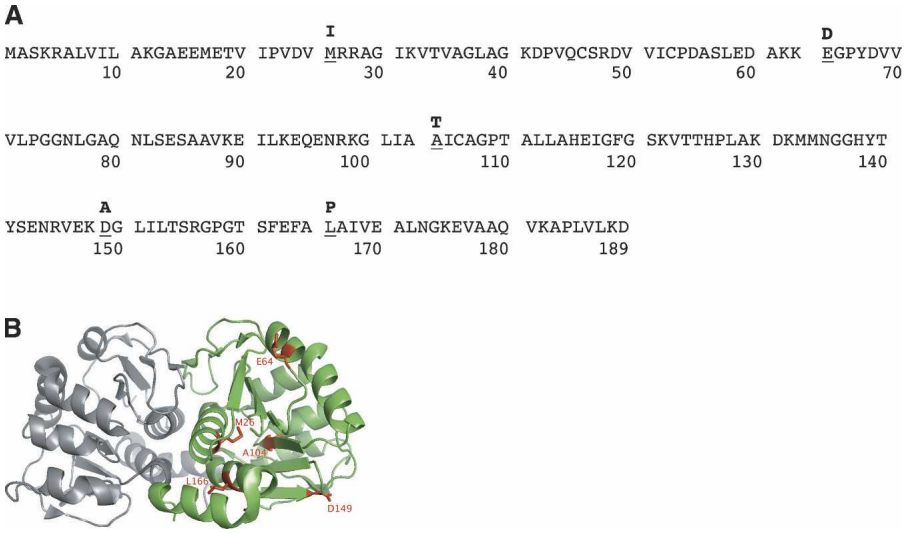

Figure 1. (*A*) Amino acid sequence of human DJ-1. Locations of disease linked mutations M26I, E64D, A104T, D149A, and L166P are underlined, with the mutations indicated in boldface *above* the wild-type sequence. (*B*) Crystal structure of the wild-type DJ-1 dimer (Wilson et al. 2003) showing one monomer in gray and the other in green. The locations of PD-linked mutations are shown and labeled in red. M26 and A104 are highly buried within the interior of the monomer; L166 is located between two helices that form part of the dimer interface; and E64 and D149 are relatively surface exposed.

M26I mutants were also able to form dimers in transfected cells, unlike L166P, but the M26I mutant exhibited a decreased ability to dimerize (Blackinton et al. 2005). In vitro the M26I mutation leads to a decrease in secondary structure, a decreased stability relative to the wild-type protein, and the formation of both an altered dimer and higher order oligomers (Hulleman et al. 2007). Here we use circular dichroism (CD) spectroscopy and solution state NMR spectroscopy to compare the structural consequences of these five PD-linked DJ-1 mutations. We find that the L166P mutant is highly and globally unfolded, consistent with its rapid degradation, inability to dimerize, and compromised function. The E64D mutant, as expected, closely resembles the wild-type protein. Interestingly, the three remaining mutants all appear to maintain the global fold of the wild-type protein, but all three exhibit a decreased thermodynamic stability as well as structural changes that propagate beyond the immediate vicinity of the mutation. These effects may therefore be expected to underlie the functional effects of these PD-linked mutations.

Results

Solution structure and dynamics of wild-type DJ-1 resemble those in the crystal state

To characterize the structural properties of wild-type DJ-1 in solution, we acquired two- and three-dimensional NMR spectra in order to permit the assignment of individual backbone resonances to their originating sites within the protein sequence. The proton-nitrogen heteronuclear single quantum coherence (HSQC) NMR spectrum of the protein, shown in Figure 2 (left panel), is annotated accordingly. The spectrum of the wild-type protein is well dispersed, occupying a chemical shift range of ~4.5 ppm and 30 ppm in the proton and nitrogen dimensions, respectively, and is typical for that of a well-folded protein. Only a single set of resonances is observed, consistent with a symmetric homodimeric structure. The presence of both widely dispersed resonances, as well as more crowded regions near the center of the spectrum are consistent with the presence of both α-helix and β-sheet structure. We analyzed the location of individual secondary structure elements within the protein sequence using a chemical shift index analysis (Wishart and Sykes 1994). The α-helix and β-strand secondary structure elements predicted based on the NMR chemical shifts are in good agreement with those observed in the crystal structure of the protein (Table 1), although the boundaries do not match precisely in every case and several two-residue strands are not identified in the chemical shift analysis, since the algorithm involved requires a minimum stretch of three residues to define a strand (the 122–123 strand is an exception in that it is identified as a four-residue strand from positions 122–125). An additional exception is α-helix 6, which extends from Lys 130 to Met 133 in the crystal structure but is not predicted by the chemical shift index. Although the shifts of residues Lys 130, Asp 131, and Lys 132 are all indicative of helical structure, that of Met 133 is not, and the algorithm requires a minimum

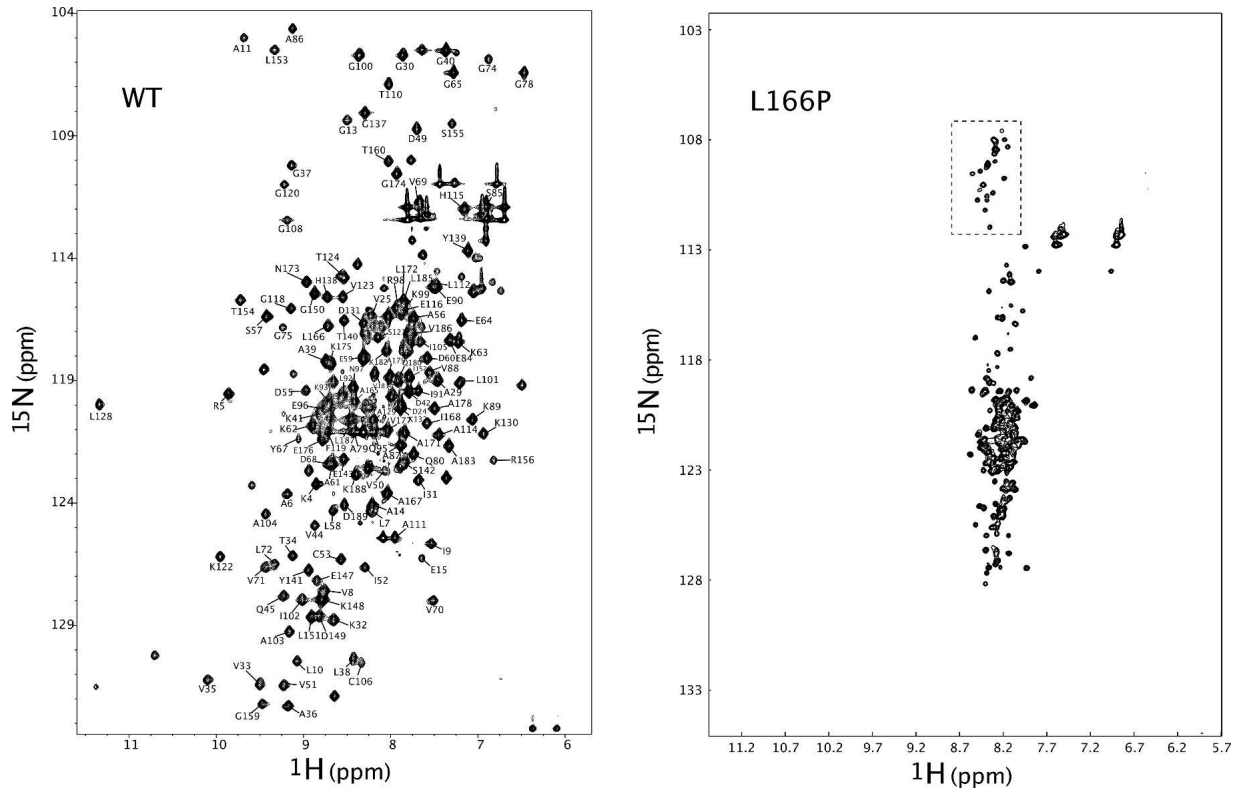

Figure 2. Proton-nitrogen correlation (HSQC) NMR spectra of wild-type (*left* panel) and L166P mutant (*right* panel) DJ-1 in 20 mM phosphate buffer, 2 mM DTT, pH 6.5 at 27°C. For the wild-type protein, good dispersion is evident in both the proton and nitrogen dimensions, consistent with a well-folded structure. The expected number of non-proline backbone amide groups (180 total) can be resolved in the spectrum, and sequence-specific resonance assignments are indicated. For the L166P mutant, poor dispersion is evident in both the proton and nitrogen dimensions, while the individual resonances are sharp and intense, indicating a poorly folded and highly flexible ensemble of structures. The dashed box in the *right* panel highlights the glycine region of the L166P spectrum.

stretch of four helical residues to define a helix. Nevertheless, the fact that three of the four shifts in this region are indicative of helix suggests that this short helix likely exists in solution as well.

To assess the dynamic properties of the wild-type protein in solution, we measured the steady-state heteronuclear [^{1}H-^{15}N] NOE (hNOE) for well-resolved backbone resonances in the two-dimensional spectrum of the protein. Values of this parameter near 1 indicate reduced librations of the NH bond vector on the picosecond-nanosecond timescale, whereas lower values indicate increasing degrees of bond vector motions. As can be seen in Figure 3 , the majority of the residues in the protein exhibit hNOE values near 1 (average value of 0.90 $\pm$ 0.09), which are typical for residues in rigid regions of well-folded proteins. Deviations from this range occur for residues at the very N and C termini, as is often seen, but also for residues 39–42, 63–67, 85, and 151–152. Residue 85 occurs at a kink between α-helix 3 and α-helix 4, whereas the remaining regions represent loops linking elements of secondary structure (β-strands 2 and 3, α-helix 2 and β-strand 5, and β-strands 10 and 11, respectively). Thus, fast timescale backbone mobility in wild-type DJ-1 occurs primarily in loops or hinges, regions that are typically somewhat mobile in well-folded proteins. To compare these results with those for DJ-1 in the crystal state, we plotted the (inverted and arbitrarily scaled) B-factor values obtained during the crystal structure determination (Wilson et al. 2003) along with the hNOE values (Fig. 3). Evidently, regions with reduced hNOE values also exhibit increased mobility in the crystal state. An exception is residue 85, for which we observed a low hNOE value but which does not exhibit a B-factor indicative of a high degree of mobility. However, α-helix 4 as a whole, extending from residue 86–97, exhibits B-factors indicating increased mobility relative to other regions of the protein, and in particular relative to α-helix 3 (residues 76–83). Thus, the mobility detected in the hNOE data for residue 85 may reflect mobility at a hinge that allows (slower) rigid body motions of α-helix 4 relative to α-helix 3.

L166P DJ-1 mutant is profoundly unfolded

Because the L166P mutation appears to have the most severe effects on the structure and stability of DJ-1, we

Table 1. *Secondary structure in wild-type DJ-1*

Secondary structure element[a]	Boundaries according to crystal structure[b]	Boundaries according to chemical shift index[c]
Strand	5–10	4–11
Helix	16–28	18–28
Strand	32–37	29–36
Helix	58–63	58–63
Strand	69–72	69–72
Helix	76–83	77–83
Helix	86–97	86–97
Strand	101–105	101–105
Strand	109–114	109–114
Strand	122–123	122–125
Helix	130–133	Not predicted
Strand	146–149	146–149
Strand	152–155	151–155
Helix	161–173	162–172
Helix	175–182	175–183

[a]Two-residue β-strands (present at residues 44–45, 51–52, 56–57, and 140–141) are not included, except for the 122–123 strand, which was detected as a four-residue strand according to chemical shift index.
[b]Determined using the Kabsch-Sander algorithm (Kabsch and Sander 1983) as implemented by the program MOLMOL (Koradi et al. 1996) applied to Protein Data Bank entry 1P5F (Wilson et al. 2003).
[c]Determined using the CSI program (Wishart and Sykes 1994).

examined the effects of this mutation first, using CD measurements of secondary structure content and thermal stability as well as two-dimensional NMR experiments. The far-UV CD spectrum of L166 DJ-1 was characteristic of a highly unfolded polypeptide, with a drastic decrease in secondary structure content compared with that of the wild-type protein (Supplemental Fig. 1), as previously reported (Olzmann et al. 2004; Shendelman et al. 2004). Nevertheless, some degree of residual helical structure is suggested by a shoulder in the spectrum around a wavelength of 222 nm. Consistent with its largely unfolded state, the L166P mutant did not exhibit a cooperative unfolding transition when the CD signal at 222 nm was measured while raising the temperature from 0°C to 96°C (Supplemental Fig. 2), as was also previously observed (Olzmann et al. 2004; Shendelman et al. 2004), but again the presence of residual structure was suggested by a slight decrease in the amplitude of the 222-nm signal at the highest temperatures. In contrast, the wild-type protein exhibits a sigmoidal unfolding transition centered at ~77°C.

The CD data clearly indicate that the L166P mutant is highly destabilized relative to the wild-type protein, but they suggest that some level of residual secondary structure remains in the mutant. This could result from the formation of transient helical and/or strand structures at different sites throughout the protein or from the presence of a small region or core that resists the destabilizing effects of the mutation and maintains a well-ordered structure while the remainder of the protein unfolds fully. To further evaluate the degree of unfolding of the L166P mutant, we compared HSQC spectra of the mutant and wild-type proteins (Fig. 2). In contrast to the spectrum of the wild-type protein, that of the L166P mutant is poorly dispersed, occupying a chemical shift range of only ~1 ppm in the proton dimension (excluding side-chain resonances) and 22 ppm in the nitrogen dimension. This low level of dispersion is typical of proteins that are largely unfolded and lacking in the tertiary interactions that provide individual residues with unique local environments. In addition, the resonances in the L166P spectrum exhibit narrower linewidths than those in the wild-type spectrum, indicating a high degree of flexibility for the L166P mutant, which is again consistent with a mostly unfolded polypeptide. Furthermore, certain regions of the spectrum exhibit more than one set of resonances. For example, the unique nitrogen chemical shift of glycine residues permits the confident identification of the 22 resonances within the dashed box in Figure 2 (right panel) as arising from glycines. There are only 18 glycine residues in the primary sequence of DJ-1 (Fig. 1A), but four of them fall immediately next to proline residues. It is likely that the additional peaks are the result of *cis*/*trans* isomerization of the Gly-Pro peptide bond, consistent with a flexible unfolded ensemble of states. The absence of any subset of well-dispersed resonances in the spectrum of L166P DJ-1 indicates that the loss of structure caused by this mutation is profound, extending throughout all regions of the protein, and that the residual secondary structure implied by the CD spectrum of this mutant does not result from a subdomain or core region that remains folded despite the destabilizing effect of the mutation.

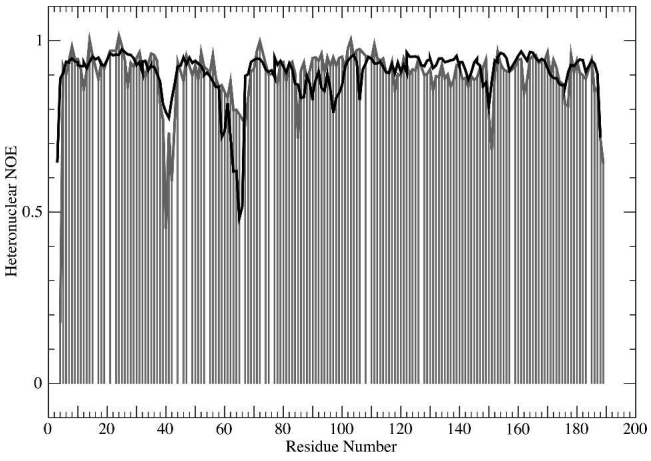

Figure 3. Backbone mobility of wild-type DJ-1 as indicated by [^{1}H-^{15}N] steady-state heteronuclear NOE values (gray) and crystallographic B-factors (black line). To facilitate the comparison, the B-factors (Wilson et al. 2003) were inverted, arbitrarily scaled, and translated. Thus, as shown, lower values in both plots indicate increased mobility.

M26I, A104T, and D149A DJ-1 mutants remain folded

The far-UV CD spectra of the M26I, A104T, and D149A DJ-1 mutants (Fig. 4) are similar in shape to that of the wild-type protein but reproducibly exhibit a decreased signal amplitude, with the effect being most pronounced for the D149A mutant. The decreased signal amplitude could result either from a perturbation in the structure of each of the mutants, or from a global destabilization that leads to an increased population of unfolded protein at equilibrium with a well-folded population. To assess whether these mutations also affect the stability of DJ-1, we monitored temperature melts of each mutant using the CD signal at 222 nm. The data (Fig. 5) reveal that all three mutations exhibit an unfolding transition at a mid-point temperature around 69°C, 8°C below that of the wild-type protein.

To further evaluate the structural effects of each of the M26I, A104T, and D149A mutations, two-dimensional NMR proton-nitrogen correlation spectra were acquired for each variant and compared with that of the wild-type protein (Fig. 6). Each of the three spectra clearly exhibits a degree of resonance dispersion equivalent to that of the wild-type protein, indicating that each mutant, like the wild type, populates a highly folded conformation with well-formed elements of α-helix and β-sheet structure. In addition to maintaining a high level of resonance dispersion, a large fraction of the resonances in the spectra of each of the three mutants are superposable with equivalent resonances in the spectrum of the wild-type protein. Because chemical shifts are exquisitely sensitive to changes in local environment, this is a strong indication that the regions of the polypeptides from which these superposable resonances arise adopt a highly similar structure in both the wild-type and mutant proteins. In contrast, where chemical shift changes are evident, they must reflect a change in the local environment of the corresponding residues. This can be caused by changes in the conformation of either these residues themselves or spatially proximal residues. To identify which regions of each mutant experience the greatest mutation-induced perturbations, we estimated the weighted average of the amide proton and nitrogen chemical shift change for each resonance in the spectrum (see Materials and Methods) and plotted the data out as a function of residue number for each mutant (Fig. 7). Clearly, in each case, resonances arising from sites immediately adjacent to the site of the mutation experience large changes in chemical shifts. In each case, however, chemical shift changes were also associated with regions that were not directly adjacent in sequence to the site of the mutation. To visualize the location of these regions relative to the mutation site in space, we mapped sites with weighted chemical shift deviations above a threshold value of 0.07 ppm onto the crystal structure of wild-type DJ-1 (Fig. 8). The threshold value was chosen heuristically based on the visual inspection of the data with the intent to include all regions that display significant chemical shift changes. In each case, chemical shift perturbations above this threshold value were found to occur for residues that were in the spatial vicinity of the mutated residue (for further discussion, see below).

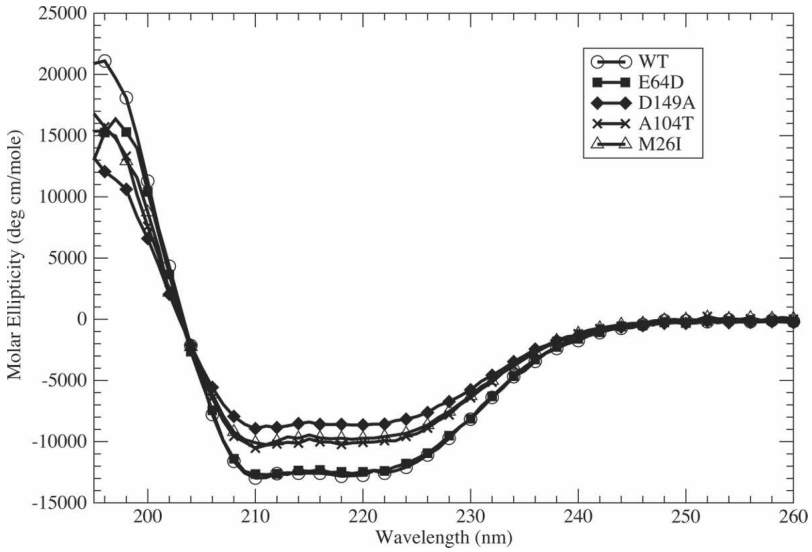

Figure 4. Circular dichroism spectra of wild-type and mutant DJ-1. The spectrum of the wild-type protein is typical of a well-structured protein containing both α-helical and β-sheet secondary structure. The spectrum of the E64D mutant is essentially identical to that of the wild-type protein. For the M26I, A104T, and D149A mutants, the spectra indicate a decrease in secondary structure content, as shown by the decreased signal at 222 nm, as well as in other spectral regions.

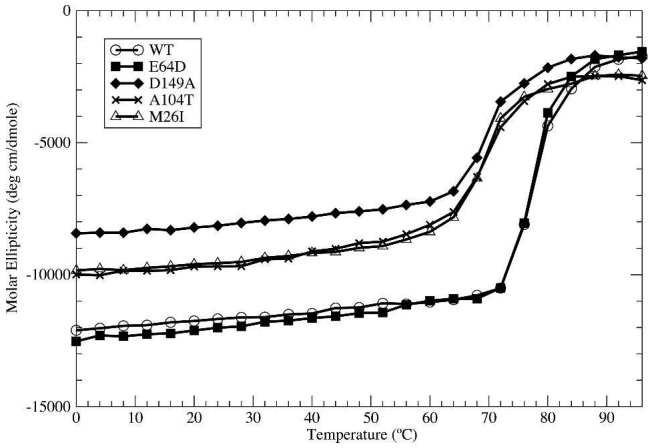

Figure 5. Temperature dependence of circular dichroism signal at 222 nm for wild-type and mutant DJ-1. The data for the wild-type protein indicate a loss of helical secondary structure with a transition midpoint of ~77°C. The E64D mutant melts at the same temperature as the wild-type protein, but the M26I, A104T, and D149A mutants melt at a temperature ~8°C below that of the wild-type protein.

E64D DJ-1 closely resembles the wild-type protein

The far-UV CD spectrum (Fig. 4), the 222-nm CD melting curve (Fig. 5), and the two-dimensional NMR proton-nitrogen correlation spectrum (Fig. 6) of the E64D DJ-1 mutant were all nearly identical to the corresponding data for the wild-type protein, confirming that the structure of this mutant is minimally perturbed. In contrast to prior reports, we do not observe either an increase (Gorner et al. 2004) or a decrease (Hulleman et al. 2007) in the thermodynamic stability of the E64D mutant. Chemical shift deviations in the two-dimensional NMR spectrum of this mutant were smaller than those observed for the other mutants and were essentially restricted to residues adjacent to the site of the mutation in the protein's primary sequence, as would be expected for a conservative mutation at a highly surface-exposed residue.

Discussion

Mutations in the protein DJ-1 are associated with a recessive form of early onset PD. Although such mutations are relatively rare as a cause of PD (Pankratz et al. 2006), they nevertheless provide an opportunity to uncover pathways that are involved in the etiology of this syndrome. To do so, it is imperative to elucidate the relevant normal functions of DJ-1, which of these normal functions are disrupted in PD, and how this disruption is caused. For PD-linked DJ-1 mutations that lead to changes in the amino acid sequence of the intact protein, functional effects are likely to be fundamentally mediated by associated changes in the physicochemical properties of the mutant proteins. To help determine the nature and extent of such changes, we studied the effects of five known PD-linked mutations on the structure and stability of DJ-1.

In general, mutations can interfere with protein function through a variety of mechanisms. At one extreme, mutations can lead to global destabilization and unfolding of a protein, which is usually associated with complete loss of function, at least for proteins that require a well-folded conformation to carry out their biological activities. At the other extreme, mutations can lead to subtle changes on a protein's surface that can modulate its interactions with binding partners in ways that compromise its function without perturbing its structure. Intermediate effects are also possible, where the conformation of a protein can be locally (or globally) altered in ways that do not lead to complete global unfolding but nevertheless perturb structural (or dynamic) properties that are crucial for function.

Our results indicate that the known PD-linked DJ-1 mutations cover the entire range of potential effects on the structure of the protein. At one extreme, the E64D DJ-1 mutation leaves the structure of the protein essentially unperturbed and appears to alter only the immediate vicinity of the mutated side chain, which is located at an exposed position on the protein surface. This is indicated by the lack of changes in the CD spectrum and melting curve of the protein (Figs. 4, 5), combined with the very limited extent of chemical shift perturbations that are observed in two-dimensional NMR spectra of this mutant (Figs. 6, 7). These results are entirely consistent with the previously determined crystal structure of this mutant, which shows no significant changes compared with the structure of the wild-type protein (Hering et al. 2004). At the other extreme, the L166P mutation leads to a severe destabilization and global unfolding of DJ-1. The CD data, in agreement with previous reports (Olzmann et al. 2004; Shendelman et al. 2004), indicate a dramatic disruption in secondary structure content, and the two-dimensional NMR spectrum of this mutant is clearly indicative of a highly disordered and flexible polypeptide chain (Fig. 2, right panel). Although this severe destabilization of the L166P leads to an increased rate of degradation in vivo (Macedo et al. 2003; Gorner et al. 2004; Olzmann et al. 2004), the degree of structural perturbation implied by our NMR spectra of L166P DJ-1 make it clear that the primary cause of the loss of function associated with this mutant is the loss of the protein's native structure and that the rapid degradation of the protein in vivo is a secondary effect.

The structural effects of the other three PD-linked DJ-1 mutants are intermediate between the extremes delineated by the E64D and L166P mutations. Unlike the L166P mutation, none of these mutations disrupt the global fold

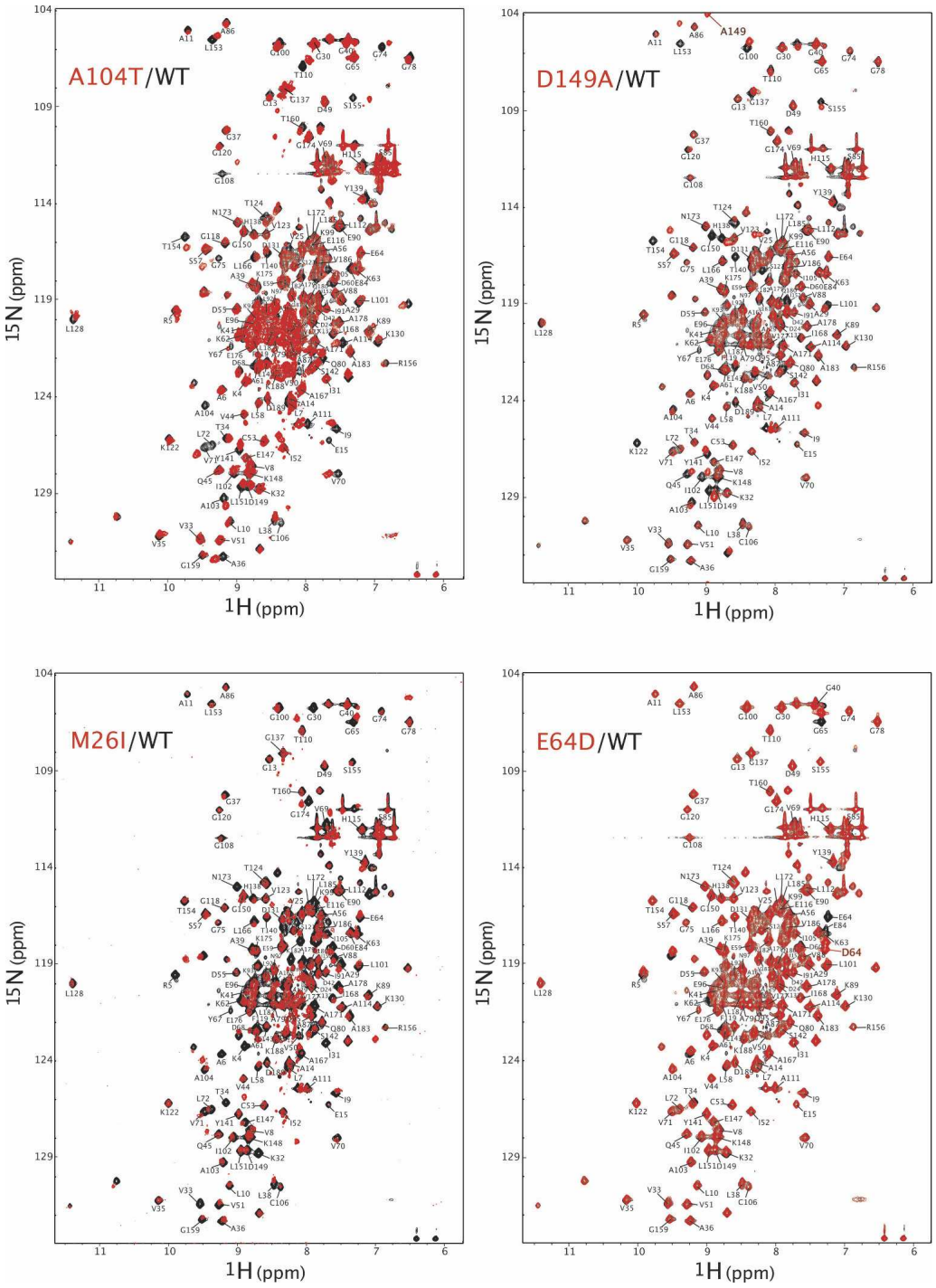

Figure 6. Overlaid proton-nitrogen correlation (HSQC) NMR spectra for wild-type (in black) and mutant (in red) DJ-1. The spectrum of the E64D mutant is nearly identical to that of the wild-type protein, with only resonances originating from the immediate vicinity of the mutation showing changes. For the M26I, A104T, and D149A mutants, the spectra exhibit a degree of dispersion comparable to, and retain a great deal of similarity to, the spectrum of the wild-type protein, suggesting that the overall structure of the protein is not dramatically altered by these mutations. Nevertheless, all three spectra reveal significant shifts in the positions of numerous resonances, many of which are not in the immediate vicinity of the mutation, indicating some degree of structural perturbation.

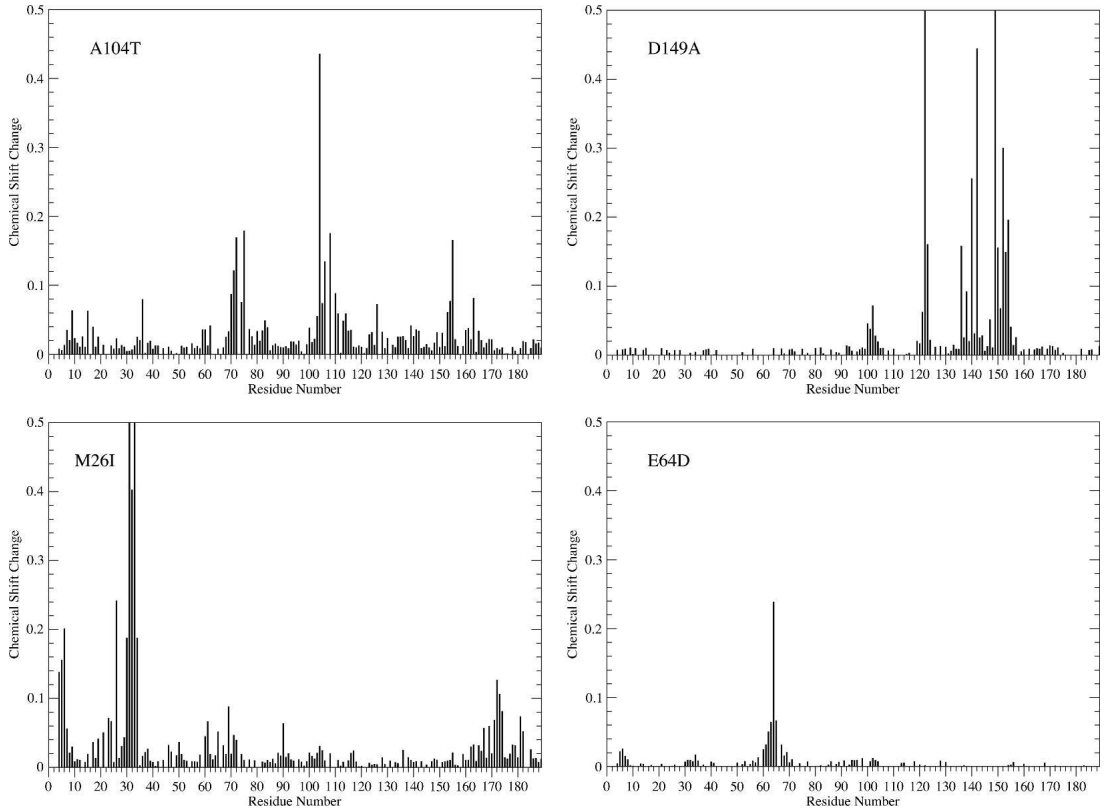

Figure 7. Weighted average of estimated chemical shift changes between the ^{1}H-^{15}N HSQC spectra of wild-type and mutant DJ-1 as a function of residue position. The weighted average of the ^{1}H and ^{15}N chemical shifts of a given residue was calculated as $[(\Delta\delta^{1}H)^{2} + (\Delta\delta^{15}N)^{2}/25]^{1/2}/2$ (Grzesiek et al. 1996).

of DJ-1. First, the CD spectra of all three mutants are similar in shape to that of the wild-type protein and clearly reflect the presence of well-formed elements of secondary structure. Furthermore, the two-dimensional NMR spectra of all three of these mutants (Fig. 6) are very similar to that of the wild-type protein and contain a large number of resonances that precisely overlap the location of corresponding resonances in the spectrum of the wild-type protein. Because of the exquisite sensitivity of NMR chemical shifts to changes in the local environment of the originating nuclei, the observed degree of similarity between the wild-type and mutant spectra is a highly reliable indication that the overall fold of the proteins is the same and is not globally perturbed. In addition, this same argument implies that all three of these mutants are dimers in solution and dimerize through the same interface observed in the crystal structure of the wild-type protein. If the mutations led to the disruption of the DJ-1 dimer, even without further perturbation of the monomer structure, residues at the dimer interface would experience a profound change in their local environment and would be expected to exhibit significant chemical shift changes. No such changes are observed for any of the mutants for resonances originating from the dimer interface (Figs. 7, 8). The conclusion that the M26I, A104T, and D149A mutants are all dimeric is consistent with previously reported pulldown assays that showed that each of these mutants is able to form both homodimers as well as heterodimers with the wild-type protein (Blackinton et al. 2005).

Given that the global structure of DJ-1 remains intact for the M26I, A104T, and D149A mutants, the decrease in secondary structure indicated in the CD spectra of the three mutants implies either that these mutations cause local perturbations of secondary structure within the protein, or possibly that they lead to a decrease in the thermodynamic stability of the protein such that the decreased CD signal reflects an equilibrium between well-folded and unfolded forms of the protein. Indeed, our CD melts demonstrate that each of the three proteins has a thermal melting temperature that is decreased by ~8°C relative to that of the wild-type protein. Nevertheless, the melting temperature of the mutants (69°C) remains far above the temperatures at which the CD and NMR spectra were acquired (27°C), and at the latter temperature, it is not expected that an appreciable fraction of

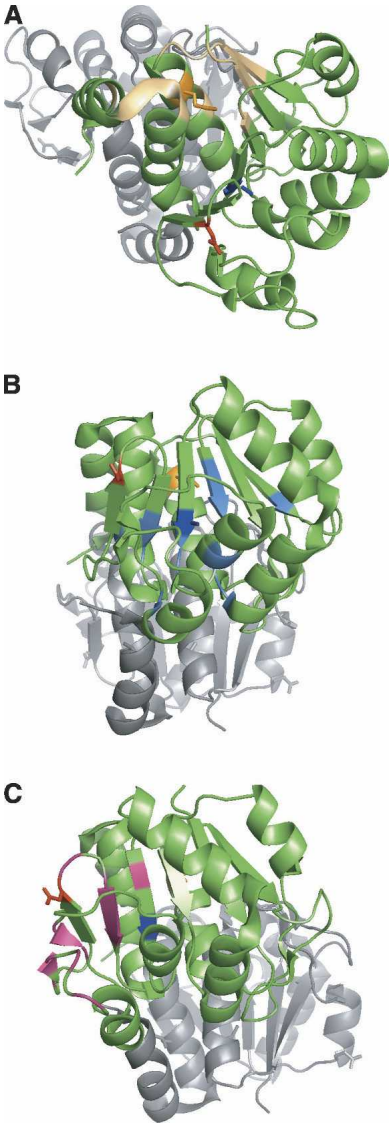

Figure 8. Chemical shift changes in DJ-1 mutants M26I (*A*), A104T (*B*), and D149A (*C*) mapped onto the structure of the wild-type protein. The location of all three mutations is shown in each panel with residue M26 in orange, A104 in dark blue, and D149 in red. Residues exhibiting weighted average chemical shift changes above a threshold value of 0.07 are highlighted in light orange for the M26I mutant, light blue for the A104T mutant, and pink for the D149A mutant. Images were created using PyMOL (DeLano Scientific; http://www.pymol.org).

unfolded protein would exist at equilibrium. In addition, if a significant population of unfolded protein existed at the conditions used for the CD and NMR experiments, this population should have been detectable as a second distinct set of signals in the NMR spectra, with dispersion properties similar to those observed for the highly unfolded L166P mutant. Since no such signals were observed in the NMR spectra, even at low contour levels (data not shown), it appears that at the temperature used here, all three of these mutants retain sufficient stability to remain well-folded. Therefore, it can be argued that the decrease in secondary structure observed in the CD spectra of all three mutants is likely caused by structural perturbations within the folded protein. Consistent with this conclusion, all three of these mutants give rise to chemical shift changes that propagate beyond residues in the immediate proximity of the site of mutation in the protein sequence, but do not indicate global unfolding.

Our knowledge of the high-resolution structure of wild-type DJ-1 allows us to identify the structural elements that are most likely perturbed by each of the mutations by mapping the locations associated with chemical shift changes onto the structure. Figure 8 shows such a mapping for each of the three mutants. In the case of the M26I mutation, which occurs in α-helix 1, residues whose associated chemical shifts are most strongly affected are found at the C-terminal end of α-helix 1 and the linker from this helix to β-strand 2, at the N-terminal ends of β-strands 1, 2, and 6, which form part of a six-stranded parallel β-sheet, in the kink between α-helices 7 and 8, and also in the middle of α-helix 8. Thus, the decrease in secondary structure associated with this mutant might be expected to result from a fraying of the C terminus of α-helix 1 and the N-terminal regions of the three affected β-strands, as well as an alteration in the C-terminal region of α-helix 7 and a part of helix 8.

The A104T mutation is found in β-strand 7 of the wild-type structure, near its C-terminal end. Chemical shift changes caused by this mutation are associated with residues in the C-terminal ends of adjacent β-strands 6, 7, and 11 of the six-stranded sheet; at the N termini of α-helices 3 and 5, which immediately follow strands 6 and 7, respectively; at the N terminus of α-helix 6; and in the middle of α-helix 7. A perturbation is also present at the C terminus of β-strand 2. In this case, perturbations localized predominantly to one half of the six-stranded β-sheet and fraying at the nearby N termini of three α-helices are expected to account for the changes observed in the CD spectrum of this mutant, although somewhat more distant residues (in strand 2 and helix 7) may be affected as well.

Residue D149 is located at the C terminus of β-strand 10, which can be considered to be either the third strand in a three-stranded antiparallel β-sheet that abuts the larger six-stranded parallel sheet (Wilson et al. 2003), or a seventh antiparallel strand at the end of the latter sheet (Tao and Tong 2003). Alteration of this residue to alanine leads to shifts in resonances originating from the two other strands in the three-stranded sheet (β-strands 8 and 9) as well as in strands 11 and 7, located at the adjacent end of the parallel sheet. The loops between α-helix 6 and β-strand 8 and between β-strands 10 and 11 are also affected. The fact that this mutation leads to perturbations

in two different β-sheets may account for the slightly greater decrease in secondary structure that is indicated by the CD spectrum of this mutant, although unlike what is observed for the other mutations, in this case there are no chemical shift perturbations associated with any elements of α-helical structure.

Because there are few reported studies of the properties of the M26I, A104T, and D149A DJ-1 mutants, there is little context in which to interpret our results. All three mutants were shown to exhibit increased rates of turnover in cells (Blackinton et al. 2005), consistent with both the structural and thermodynamic destabilization that we have documented here, but the M26I turnover rate was significantly higher than for A104T and D149A, although not as high as for the L166P mutant. For the M26I mutant, a recent report also indicated a decreased level of secondary structure as seen by CD, in agreement with our own results (Hulleman et al. 2007). This study also showed, using size exclusion chromatography, that M26I is capable of forming dimers. Although the authors did not observe any heat denaturation of the M26I mutant by CD, in contrast with our own results, they did establish that this mutant is thermodynamically destabilized using chemical denaturant melts. The same study also noted that the M26I mutant has a higher propensity to oligomerize than the wild-type protein. In agreement with this result, we did observe that our M26I NMR samples were unstable over a timescale of several days, with the formation of a visible precipitate accompanying significant degradation in spectral quality. With regard to the A104T or D149A DJ-1 mutations, prior to our own work reported here, no such information has been reported. For all three of these ''intermediate'' mutations, no functional studies have been reported.

Despite the absence of specific information about functional changes caused by the M26I, A104T, and D149A mutations, our results can be combined with what is known about the functions of wild-type DJ-1 to propose how these mutations might inactivate such functions. Both the chaperone and antioxidant proposed functions of DJ-1 appear to depend on oxidation/reduction of Cys 106 of the protein. Cys 106 is located just C-terminal to the end of β-strand 7, in close proximity to the antiparallel three-stranded sheet, the N termini of helices 6 and 7, and the C termini of β-strands 6, 7, and 11 of the six-stranded sheet. These structural elements are precisely the ones affected by the A104T and D149A mutations, as discussed above, and we therefore conjecture that these mutations compromise DJ-1 function by locally perturbing the protein geometry surrounding Cys 106 in such a way as to interfere with proper involvement of this residue in the function of the protein. In contrast, the M26I mutation affects structural elements that are relatively distant from Cys 106, and such a mechanism is less likely to be the basis of DJ-1 inactivation by this mutation. Instead, we propose that in the case of M26I, a perturbation of structure in α-helix 1, which is a central feature of the DJ-1 dimer interface, disrupts the contacts at this interface and leads to the previously noted decrease in the stability of the dimer (Hulleman et al. 2007). This decreased dimer stability is, in turn, likely responsible both for the aggregation/precipitation observed by ourselves and Hulleman et al. (2007) as well as for the greatly increased turnover time of this mutant in cells relative to all other mutants save the highly unfolded L166P variant. Thus, the M26I mutant can form dimers, which based on the lack of structural perturbation near Cys 106 may be functional, but the instability of these dimers leads to aggregation and/or clearance of the protein, which we then propose is the fundamental cause of the loss of function of this DJ-1 mutant.

While the work presented here was under review, an article appeared describing the crystal structures of the M26I and A104T DJ-1 mutants (Lakshminarasimhan et al. 2008). The results are largely consistent with those described here. In particular, both mutant proteins adopt dimeric structures in which the global fold of the wild-type protein is closely preserved, in agreement with our conclusions based on the NMR data. Furthermore, the sites observed to be most clearly perturbed in the crystal structures of the mutants correspond to the regions with the greatest chemical shift changes in the NMR spectra of the mutants. Specifically, the A104T crystal structure shows significant (~0.4 Å) displacements of residues L72 and L112, which are in those regions that show the greatest chemical shift deviations, aside from the site of the mutation itself (Fig. 7). Notably, the position of residue T154 is also slightly perturbed, and this is clearly reflected in the chemical shift data as well. The M26I structure shows an even larger (~0.7 Å) displacement for residue I31, which falls into the region exhibiting the largest chemical shift changes observed for any of the well-folded mutants in our study. An analysis using the program PROCOMPARE (part of the PROCHECK program suite) (Laskowski et al. 1993) shows additional changes in the backbone dihedral angles of residues 32 and 33, consistent with large chemical shift changes at these sites, as well as smaller dihedral angle changes for residues 4 and 5, in accordance with smaller chemical shift deviations in this region. For both mutants, the chemical shift data delineate smaller changes at a number of other sites that are not obviously perturbed in the crystal structures. This likely reflects the exquisite sensitivity of chemical shifts to local environment and their ability to reflect changes that may be difficult to discern in crystal structures, even at high resolution. One significant difference between our results and those obtained based on the recent crystal structures is in the secondary

structure content of the M26I and A104T mutants. In contrast to the partial loss of secondary structure implied by our CD data, the secondary structure elements of both mutants are fully intact in the crystal structures and are essentially identical to those of the wild-type protein. Although it is possible that partial oxidation of Cys 106 in our samples, as reported in prior studies (Hulleman et al. 2007), might be responsible for this difference, this would be expected to give rise to chemical shift changes around Cys 106 and we do not observe such changes for the M26I mutant in particular (Fig. 7). Alternate possible explanations for this disagreement may include the potentially stabilizing effects of crystal lattice packing or differences in the conditions used in the two studies.

Conclusions

This work provides a comprehensive comparison of the physicochemical properties of five PD-linked DJ-1 mutants and both complements and extends previous results obtained for different individual mutations. By combining CD and NMR spectroscopy to study the effects of these mutations on the structure and stability of DJ-1, we have proposed different mechanisms by which each of the mutations likely leads to a loss of DJ-1 function. We first established that the structure and dynamics of the wild-type protein in solution closely resemble those observed in its crystal structure. For the E64D mutation, our results confirm the previously noted absence of any significant structural changes but, in contrast to other work, indicate that no significant change in thermodynamic stability occurs either. We therefore suggest that this mutation most likely alters interactions of DJ-1 with other cellular partners that are crucial for proper execution of its function(s). For the L166P mutation, our results reveal that the extent of the previously noted structural disruption of this mutant is profound in that no regions of stable structure persist within this mutant. Thus, this mutation leads to a highly unfolded form of the protein that no longer possesses the structural features needed to carry out its function(s). The increased clearance and decreased steady-state levels of this protein in cells are not the primary cause of the loss of function exhibited by this mutant, and are instead, a secondary consequence of the observed loss of structure. In the case of the A104T and D149A mutations, we show that both mutant proteins adopt the dimeric wild-type fold and that many aspects of their structures are essentially identical to those of the wild-type protein. However, both of these mutations lead to local structural perturbations in the spatial vicinity of residue Cys 106, a likely key mediator of DJ-1 function, and these perturbations may therefore preclude formation of the requisite functional local geometry around this residue. We find that the M26I mutant is also able to adopt the dimeric wild-type fold, and in this instance, the vicinity of residue Cys106 is not directly perturbed, suggesting that this mutant may in fact be functional. However, chemical shift changes in charged residues near M26 may reflect alterations that influence Cys 106 oxidation and thereby underlie the reported effects of this mutation on the stability of the oxidized form of the protein (Hulleman et al. 2007). In either case, this mutation interferes with structural elements that are key components of the DJ-1 dimer interface, and appears thereby to destabilize this interface, causing the protein to dissociate more easily and subsequently to aggregate. In cells, this effect is accompanied by a greatly increased rate of clearance of this mutant, which we propose is the primary cause of the associated loss of function in this case. Testing these hypotheses will require further experiments, both to characterize in greater detail the structure and dynamics of the mutants, and to characterize more fully their functional effects in situ and in vivo. Ultimately, an improved understanding of how DJ-1 inactivation takes place in, and contributes to, PD should emerge.

Materials and Methods

Expression and purification of isotopically labeled DJ-1and its mutants

We utilized a previously constructed pET24d plasmid construct (Tao and Tong 2003) generously provided by Dr. Liang Tong (Department of Biological Sciences, Columbia University, New York) containing the cDNA sequence of wild-type DJ-1 fused to a C-terminal hexa-histidine tag. The QuikChange site directed mutagenesis kit (Stratagene) was used to produce plasmids encoding the PD-linked DJ-1 mutants M26I, E64D A104T, D149A, and L166P. All constructs were verified by DNA sequencing. Recombinant proteins were overexpressed in *Escherichia coli* at 37°C using IPTG to induce cultures at mid-log phase (OD_{600} of 0.6). To produce isotopically labeled samples for NMR studies, single colonies were inoculated into M9 minimal media containing ammonium chloride as the sole source of nitrogen and dextrose as the sole source of carbon. ^{15}N-enriched ammonium chloride (1 g/L) was used to produce uniformly ^{15}N-labeled proteins, and ^{13}C-enriched dextrose (2 g/L) was additionally used to produce uniformly ^{13}C,^{15}N-labeled proteins. For production of fractionally deuterated proteins, cultures were grown in media made using 99% D_2O (Cambridge Isotope). Cells were harvested by centrifugation after 4 h, and proteins were purified using a standard protocol. In brief, cells were subjected to one cycle of freeze- thaw in lysis buffer (10 mM Tris, 1 mM EDTA, 1mM DTT, 1mM PMSF, pH 8.0) and sonicated on ice, followed by ultracentrifugation to pellet insoluble cell debris. DJ-1 and all mutants were found in the soluble fraction. The supernatant was subjected to two ammonium sulfate cuts (0.116 g/mL followed by an additional 0.129 g/mL), and the resulting supernatant was applied to a nickel affinity column, which was thoroughly equilibrated with lysis buffer, washed (350 mM NaCl, 20 mM imidazole, 20 mM Tris, 1.5 mM BME, 2 mM DTT, pH 8.0), and eluted with an imidazole gradient (up to 250 mM imidazole in wash buffer). SDS-PAGE was used to locate DJ-1–containing fractions, which

were pooled, applied to a DEAE anion exchange column (equilibrated with 25 mM Tris, 20 mM NaCl, 1 mM EDTA, 1 mM DTT, pH 6), and eluted with a NaCl gradient (up to 1 M NaCl in equilibration buffer). Protein containing fractions were pooled, concentrated, and dialyzed against 20 mM sodium phosphate, 2 mM DTT, pH 6.0. Protein purity was assessed to be greater that 95% using SDS-PAGE (Supplemental Fig. 3), and mass spectrometry was used to verify the identity, purity, and isotopic labeling of the protein. Only freshly prepared samples were used in all experiments. Protein concentrations were obtained from measurements of absorption at 280 nm using an extinction coefficient of 4207.8, initially determined using a BCA Protein Assay (Pierce). Typical protein concentrations were 50 μM for CD experiments and 250 μM for NMR experiments.

Circular dichroism

CD spectra were acquired on an AVIV 62 DS spectrometer equipped with a sample temperature controller. Far-UV CD spectra were monitored from 190 to 260 nm with a step size of 1 nm and response time of 4 sec, using a 0.2-mm path-length quartz cuvette at 27°C. Each spectrum is the average of five scans. Thermal denaturation measurements were performed in the same cuvette at a wavelength of 222 nm in 4°C increments from 0°C to 96°C with an equilibration time of 1 min and an integration time of 30 sec. All CD spectra and melting curves were acquired in at least two independent measurements to ensure reproducibility, and representative data are presented in the figures.

NMR

Triple-resonance NMR experiments (HNCACB, CBCACONH, HN(CA)CO, and HNCO) and measurements of the steady-state [^{1}H-^{15}N] NOE were performed using TROSY versions with fractionally deuterated protein samples on a 900-MHz Bruker instrument at the New York Structural Biology Center. Proton-nitrogen correlation spectra of the DJ-1 variants were acquired on a 600-MHz Varian instrument at the Weill Cornell Medical College NMR facility. All spectra were collected at a temperature of 27°C. Spectral widths of 14, 40, 65, and 20 ppm were used for the proton, nitrogen, Cα/Cβ, and CO dimensions, respectively. Spectra were processed using NMRPipe (Delaglio et al. 1995) and analyzed using NMRView (Johnson and Blevins 1994). Steady-state heteronuclear NOE measurements were performed using 4 sec of proton saturation applied (or not) during a 5-sec relaxation interval. Three pairs of spectra (with and without saturation) were acquired, and the variance in the resonance intensity ratios was used to estimate errors.

Resonance assignments for backbone NH, ^{15}N, Cα, and CO, as well as Cβ nuclei were obtained for the wild-type protein using inter-residue connectivities observed in triple-resonance experiments. Based on the Cβ chemical shifts of all three DJ-1 cysteine residues (27.99, 27.55, and 27.51 ppm for Cys 46, 53, and 106, respectively) and the lack of any doubling of the Cys resonances, samples were confirmed to be fully reduced. To estimate the chemical shift changes induced by the PD-linked M26I, E64D, A104T, and D149A mutations, tentative assignments of the proton-nitrogen correlation spectrum of each mutant were obtained by transferring each previously obtained wild-type resonance assignment to the nearest resonance in the spectra of the mutant proteins, unless that resonance had already been assigned to a (nearer) wild-type resonance, in which case the next nearest resonance was considered. While this strategy does not guarantee correct assignments, it will in general underestimate the chemical shift change in those cases where the assignments are incorrect. Thus, where chemical shift deviations are observed using this method, they can be considered to reliably indicate changes in the local environment of the originating residue. To assess such changes, the weighted average of the amide proton and nitrogen chemical shift changes between each mutant and the wild-type protein were calculated according to the formula $[(\Delta\delta^{1}H)^{2} + (\Delta\delta^{15}N)^{2}/25]^{1/2}/2$ (Grzesiek et al. 1996).

Electronic supplemental material

Supplemental material contains three figures showing CD data comparing the L166P mutant with wild-type DJ-1 and an SDS-PAGE gel of purified DJ-1.

Acknowledgments

We thank Dr. Liang Tong and Dr. Asa Abeliovich (Columbia University) for their kind gifts of DJ-1 expression vectors and Mike Goger, Kaushik Dutta, and Shibani Bhattacharya (NYSBC) for support related to NMR data collection and processing. D.E. is a member of the New York Structural Biology Center, which is a STAR center supported by the New York State Office of Science, Technology and Academic Research; is supported by NIH grant P41 GM66354; and received funds from NIH, USA, the Keck Foundation, New York State, and the NYC Economic Development Corporation for the purchase of 900-MHz spectrometers. D.E. also acknowledges support from the Irma T. Hirschl Foundation and a gift from Herbert and Ann Siegel.

References

Abou-Sleiman, P.M., Healy, D.G., Quinn, N., Lees, A.J., and Wood, N.W. 2003. The role of pathogenic DJ-1 mutations in Parkinson's disease. *Ann. Neurol.* **54:** 283–286.

Andres-Mateos, E., Perier, C., Zhang, L., Blanchard-Fillion, B., Greco, T.M., Thomas, B., Ko, H.S., Sasaki, M., Ischiropoulos, H., Przedborski, S., et al. 2007. DJ-1 gene deletion reveals that DJ-1 is an atypical peroxiredoxin-like peroxidase. *Proc. Natl. Acad. Sci.* **104:** 14807–14812.

Annesi, G., Savettieri, G., Pugliese, P., D'Amelio, M., Tarantino, P., Ragonese, P., La Bella, V., Piccoli, T., Civitelli, D., Annesi, F., et al. 2005. DJ-1 mutations and parkinsonism-dementia-amyotrophic lateral sclerosis complex. *Ann. Neurol.* **58:** 803–807.

Betarbet, R., Canet-Aviles, R.M., Sherer, T.B., Mastroberardino, P.G., McLendon, C., Kim, J.H., Lund, S., Na, H.M., Taylor, G., Bence, N.F., et al. 2006. Intersecting pathways to neurodegeneration in Parkinson's disease: Effects of the pesticide rotenone on DJ-1, α-synuclein, and the ubiquitin-proteasome system. *Neurobiol. Dis.* **22:** 404–420.

Blackinton, J., Ahmad, R., Miller, D.W., van der Brug, M.P., Canet-Aviles, R.M., Hague, S.M., Kaleem, M., and Cookson, M.R. 2005. Effects of DJ-1 mutations and polymorphisms on protein stability and subcellular localization. *Brain Res. Mol. Brain Res.* **134:** 76–83.

Bonifati, V., Rizzu, P., van Baren, M.J., Schaap, O., Breedveld, G.J., Krieger, E., Dekker, M.C., Squitieri, F., Ibanez, P., Joosse, M., et al. 2003. Mutations in the DJ-1 gene associated with autosomal recessive early-onset parkinsonism. *Science* **299:** 256–259.

Canet-Aviles, R.M., Wilson, M.A., Miller, D.W., Ahmad, R., McLendon, C., Bandyopadhyay, S., Baptista, M.J., Ringe, D., Petsko, G.A., and Cookson, M.R. 2004. The Parkinson's disease protein DJ-1 is neuroprotective due to cysteine-sulfinic acid-driven mitochondrial localization. *Proc. Natl. Acad. Sci.* **101:** 9103–9108.

Delaglio, F., Grzesiek, S., Vuister, G.W., Zhu, G., Pfeifer, J., and Bax, A. 1995. NMRPipe: A multidimensional spectral processing system based on UNIX pipes. *J. Biomol. NMR* **6:** 277–293.

Gorner, K., Holtorf, E., Odoy, S., Nuscher, B., Yamamoto, A., Regula, J.T., Beyer, K., Haass, C., and Kahle, P.J. 2004. Differential effects of Parkinson's disease-associated mutations on stability and folding of DJ-1. *J. Biol. Chem.* **279:** 6943–6951.

Grzesiek, S., Bax, A., Clore, G.M., Gronenborn, A.M., Hu, J.S., Kaufman, J., Palmer, I., Stahl, S.J., and Wingfield, P.T. 1996. The solution structure of HIV-1 Nef reveals an unexpected fold and permits delineation of the binding surface for the SH3 domain of Hck tyrosine protein kinase. *Nat. Struct. Biol.* **3:** 340–345.

Hague, S., Rogaeva, E., Hernandez, D., Gulick, C., Singleton, A., Hanson, M., Johnson, J., Weiser, R., Gallardo, M., Ravina, B., et al. 2003. Early-onset Parkinson's disease caused by a compound heterozygous DJ-1 mutation. *Ann. Neurol.* **54:** 271–274.

Hering, R., Strauss, K.M., Tao, X., Bauer, A., Woitalla, D., Mietz, E.M., Petrovic, S., Bauer, P., Schaible, W., Muller, T., et al. 2004. Novel homozygous p.E64D mutation in DJ1 in early onset Parkinson disease (PARK7). *Hum. Mutat.* **24:** 321–329.

Hod, Y., Pentyala, S.N., Whyard, T.C., and El-Maghrabi, M.R. 1999. Identification and characterization of a novel protein that regulates RNA-protein interaction. *J. Cell. Biochem.* **72:** 435–444.

Honbou, K., Suzuki, N.N., Horiuchi, M., Niki, T., Taira, T., Ariga, H., and Inagaki, F. 2003. The crystal structure of DJ-1, a protein related to male fertility and Parkinson's disease. *J. Biol. Chem.* **278:** 31380–31384.

Huai, Q., Sun, Y., Wang, H., Chin, L.S., Li, L., Robinson, H., and Ke, H. 2003. Crystal structure of DJ-1/RS and implication on familial Parkinson's disease. *FEBS Lett.* **549:** 171–175.

Hulleman, J.D., Mirzaei, H., Guigard, E., Taylor, K.L., Ray, S.S., Kay, C.M., Regnier, F.E., and Rochet, J.C. 2007. Destabilization of DJ-1 by familial substitution and oxidative modifications: Implications for Parkinson's disease. *Biochemistry* **46:** 5776–5789.

Johnson, B.A. and Blevins, R.A. 1994. NMRView: A computer program for the visualization and analysis of NMR data. *J. Biomol. NMR* **4:** 603–614.

Kabsch, W. and Sander, C. 1983. Dictionary of protein secondary structure: Pattern recognition of hydrogen-bonded and geometrical features. *Biopolymers* **22:** 2577–2637.

Kim, R.H., Smith, P.D., Aleyasin, H., Hayley, S., Mount, M.P., Pownall, S., Wakeham, A., You-Ten, A.J., Kalia, S.K., Horne, P., et al. 2005. Hypersensitivity of DJ-1-deficient mice to 1-methyl-4-phenyl-1,2,3,6-tetrahydropyridine (MPTP) and oxidative stress. *Proc. Natl. Acad. Sci.* **102:** 5215–5220.

Kitada, T., Asakawa, S., Hattori, N., Matsumine, H., Yamamura, Y., Minoshima, S., Yokochi, M., Mizuno, Y., and Shimizu, N. 1998. Mutations in the parkin gene cause autosomal recessive juvenile parkinsonism. *Nature* **392:** 605–608.

Koradi, R., Billeter, M., and Wuthrich, K. 1996. MOLMOL: A program for display and analysis of macromolecular structures. *J. Mol. Graph.* **14:** 29–32, 51–55.

Lakshminarasimhan, M., Maldonado, M.T., Zhou, W., Fink, A.L., and Wilson, M.A. 2008. Structural impact of three Parkinsonism-associated missense mutations on human DJ-1. *Biochemistry* **47:** 1381–1392.

Laskowski, R.A., MacArthur, M.W., Moss, D.S., and Thornton, J.M. 1993. PROCHECK: A program to check the stereochemical quality of protein structures. *J. Appl. Crystallogr.* **26:** 283–291.

Lavara-Culebras, E. and Paricio, N. 2007. *Drosophila* DJ-1 mutants are sensitive to oxidative stress and show reduced lifespan and motor deficits. *Gene* **400:** 158–165.

Lee, S.J., Kim, S.J., Kim, I.K., Ko, J., Jeong, C.S., Kim, G.H., Park, C., Kang, S.O., Suh, P.G., Lee, H.S., et al. 2003. Crystal structures of human DJ-1 and *Escherichia coli* Hsp31, which share an evolutionarily conserved domain. *J. Biol. Chem.* **278:** 44552–44559.

Macedo, M.G., Anar, B., Bronner, I.F., Cannella, M., Squitieri, F., Bonifati, V., Hoogeveen, A., Heutink, P., and Rizzu, P. 2003. The DJ-1L166P mutant protein associated with early onset Parkinson's disease is unstable and forms higher-order protein complexes. *Hum. Mol. Genet.* **12:** 2807–2816.

Martinat, C., Shendelman, S., Jonason, A., Leete, T., Beal, M.F., Yang, L., Floss, T., and Abeliovich, A. 2004. Sensitivity to oxidative stress in DJ-1-deficient dopamine neurons: An ES-derived cell model of primary Parkinsonism. *PLoS Biol.* **2:** e327. doi: 10.1371/journal.pbio.0020327.

Miller, D.W., Ahmad, R., Hague, S., Baptista, M.J., Canet-Aviles, R., McLendon, C., Carter, D.M., Zhu, P.P., Stadler, J., Chandran, J., et al. 2003. L166P mutant DJ-1, causative for recessive Parkinson's disease, is degraded through the ubiquitin-proteasome system. *J. Biol. Chem.* **278:** 36588–36595.

Mitsumoto, A. and Nakagawa, Y. 2001. DJ-1 is an indicator for endogenous reactive oxygen species elicited by endotoxin. *Free Radic. Res.* **35:** 885–893.

Mitsumoto, A., Nakagawa, Y., Takeuchi, A., Okawa, K., Iwamatsu, A., and Takanezawa, Y. 2001. Oxidized forms of peroxiredoxins and DJ-1 on two-dimensional gels increased in response to sub-lethal levels of paraquat. *Free Radic. Res.* **35:** 301–310.

Moore, D.J., Zhang, L., Dawson, T.M., and Dawson, V.L. 2003. A missense mutation (L166P) in DJ-1, linked to familial Parkinson's disease, confers reduced protein stability and impairs homo-oligomerization. *J. Neurochem.* **87:** 1558–1567.

Olzmann, J.A., Brown, K., Wilkinson, K.D., Rees, H.D., Huai, Q., Ke, H., Levey, A.I., Li, L., and Chin, L.S. 2004. Familial Parkinson's disease-associated L166P mutation disrupts DJ-1 protein folding and function. *J. Biol. Chem.* **279:** 8506–8515.

Paisan-Ruiz, C., Jain, S., Evans, E.W., Gilks, W.P., Simon, J., van der Brug, M., Lopez de Munain, A., Aparicio, S., Gil, A.M., Khan, N., et al. 2004. Cloning of the gene containing mutations that cause PARK8-linked Parkinson's disease. *Neuron* **44:** 595–600.

Pankratz, N., Pauciulo, M.W., Elsaesser, V.E., Marek, D.K., Halter, C.A., Wojcieszek, J., Rudolph, A., Shults, C.W., Foroud, T., and Nichols, W.C. 2006. Mutations in DJ-1 are rare in familial Parkinson disease. *Neurosci. Lett.* **408:** 209–213.

Polymeropoulos, M.H., Lavedan, C., Leroy, E., Ide, S.E., Dehejia, A., Dutra, A., Pike, B., Root, H., Rubenstein, J., Boyer, R., et al. 1997. Mutation in the α-synuclein gene identified in families with Parkinson's disease. *Science* **276:** 2045–2047.

Ramirez, A., Heimbach, A., Grundemann, J., Stiller, B., Hampshire, D., Cid, L.P., Goebel, I., Mubaidin, A.F., Wriekat, A.L., Roeper, J., et al. 2006. Hereditary parkinsonism with dementia is caused by mutations in ATP13A2, encoding a lysosomal type 5 P-type ATPase. *Nat. Genet.* **38:** 1184–1191.

Shendelman, S., Jonason, A., Martinat, C., Leete, T., and Abeliovich, A. 2004. DJ-1 is a redox-dependent molecular chaperone that inhibits α-synuclein aggregate formation. *PLoS Biol.* **2:** e362. doi: 10.1371/journal.pbio.0020362.

Taira, T., Saito, Y., Niki, T., Iguchi-Ariga, S.M., Takahashi, K., and Ariga, H. 2004. DJ-1 has a role in antioxidative stress to prevent cell death. *EMBO Rep.* **5:** 213–218.

Tang, B., Xiong, H., Sun, P., Zhang, Y., Wang, D., Hu, Z., Zhu, Z., Ma, H., Pan, Q., Xia, J.H., et al. 2006. Association of PINK1 and DJ-1 confers digenic inheritance of early-onset Parkinson's disease. *Hum. Mol. Genet.* **15:** 1816–1825.

Tao, X. and Tong, L. 2003. Crystal structure of human DJ-1, a protein associated with early onset Parkinson's disease. *J. Biol. Chem.* **278:** 31372–31379.

Valente, E.M., Abou-Sleiman, P.M., Caputo, V., Muqit, M.M., Harvey, K., Gispert, S., Ali, Z., Del Turco, D., Bentivoglio, A.R., Healy, D.G., et al. 2004. Hereditary early-onset Parkinson's disease caused by mutations in PINK1. *Science* **304:** 1158–1160.

Wagenfeld, A., Gromoll, J., and Cooper, T.G. 1998. Molecular cloning and expression of rat contraception associated protein 1 (CAP1), a protein putatively involved in fertilization. *Biochem. Biophys. Res. Commun.* **251:** 545–549.

Wilson, M.A., Collins, J.L., Hod, Y., Ringe, D., and Petsko, G.A. 2003. The 1.1-Å resolution crystal structure of DJ-1, the protein mutated in autosomal recessive early onset Parkinson's disease. *Proc. Natl. Acad. Sci.* **100:** 9256–9261.

Wishart, D.S. and Sykes, B.D. 1994. The 13C chemical-shift index: A simple method for the identification of protein secondary structure using ^{13}C chemical-shift data. *J. Biomol. NMR* **4:** 171–180.

Zhou, W., Zhu, M., Wilson, M.A., Petsko, G.A., and Fink, A.L. 2006. The oxidation state of DJ-1 regulates its chaperone activity toward α-synuclein. *J. Mol. Biol.* **356:** 1036–1048.

Zimprich, A., Biskup, S., Leitner, P., Lichtner, P., Farrer, M., Lincoln, S., Kachergus, J., Hulihan, M., Uitti, R.J., Calne, D.B., et al. 2004. Mutations in LRRK2 cause autosomal-dominant parkinsonism with pleomorphic pathology. *Neuron* **44:** 601–607.